Molecular Pharmacology Fast Forward. Published on March 29, 2006 as doi:10.1124/mol.105.021204

Mol Manuscript # 21204

IDENTIFICATION OF TUBULIN AS THE MOLECULAR TARGET OF PRO-APOPTOTIC PYRROLO-1,5-BENZOXAZEPINES

JUDE M. MULLIGAN, LISA M. GREENE, SUZANNE CLOONAN, MARGARET M. MC GEE, VALERIA ONNIS, GIUSEPPE CAMPIANI, CATERINA FATTORUSSO, MARK LAWLER, D. CLIVE WILLIAMS AND DANIELA M. ZISTERER

School of Biochemistry and Immunology, Trinity College, Dublin 2, Ireland, JMM, LMG, SC, VO, DCW, DMZ; Conway Institute of Molecular and Biomedical Research, University College Dublin, Belfield, Dublin 4, Ireland, MMM; Dipartimento Farmaco Chimico Tecnologico, Universita' degli Studi di Siena, Siena, Italy, GC, CF; The Institute of Molecular Medicine, St James's Hospital and Trinity College, Dublin 2, Ireland, ML.

Molecular Pharmacology Fast Forward. Published on March 29, 2006 as DOI: 10.1124/mol.105.021204
This article has not been copyedited and formatted. The final version may differ from this version.

Running Title: Pyrrolobenzoxazepines and microtubule targeting drugs

Abbreviations: Pyrrolo-1,5-benzoxazepine (PBOX), Cyclin Dependent Kinase (CDK), c-Jun-N-terminal kinase (JNK), European Collection of Cell Cultures (ECACC), Minimum Essential Medium (MEM), Roswell Park Memorial Institute Medium (RPMI), Fluorescein Isothiocyanate (FITC), Poly ADP-Ribose Polymerase (PARP), Glutathione-*S*-Transferase (GST), Foetal Calf Serum (FCS), Phosphate-Buffered Saline (PBS), Immunoprecipitation (IP), Dithiothreitol (DTT), Phenylmethanesulfonyl Fluoride (PMSF), Sodium dodecyl sulphate (SDS), Polyacrylamide gel electrophoresis (PAGE), Polyvinyldifluoride (PVDF), Tris-Buffered Saline (TBS), Bovine Serum Albumin (BSA), Propidium Iodide (PI), Guanosine Triphosphate (GTP), Fluorescence-Activated Cell Sorter (FACS), Chronic Myelogenous Leukemia (CML), Dimethyl Sulfoxide (DMSO).

Corresponding author: Dr Daniela Zisterer, Tel: 00 353 1 6081628, Fax: 00 353 1 6772400, Email: **dzistrer@tcd.ie**

Pages: 24

Tables: 0

Figures: 8

References: 39

Words in Abstract: 248

Words in Introduction: 697

Words in Discussion: 1,454

Molecular Pharmacology Fast Forward. Published on March 29, 2006 as DOI: 10.1124/mol.105.021204
This article has not been copyedited and formatted. The final version may differ from this version.

ABSTRACT

This group has previously demonstrated that certain members of a series of novel PBOX compounds potently induce apoptosis in a variety of human chemotherapy resistant cancer cell lines and in primary *ex vivo* derived material from cancer patients. A better understanding of the molecular mechanisms underlying the apoptotic effects of these PBOX compounds is essential to their development as anti-neoplastic therapeutic agents. This study sought to test the hypothesis that pro-apoptotic PBOX compounds target the microtubules. We show that a representative pro-apoptotic PBOX compound, PBOX-6, induces apoptosis in both the MCF-7 and K562 cell lines. An accumulation of cells in G2/M precedes apoptosis in response to PBOX-6. PBOX-6 induces prometaphase arrest and causes an accumulation of cyclin B_1 levels and activation of cyclin B_1/CDK1 kinase in a manner similar to two representative anti-microtubule agents, nocodazole and paclitaxel. Indirect immunofluorescence demonstrates that both PBOX-6 and another pro-apoptotic PBOX compound, PBOX-15, cause microtubule depolymerisation in MCF-7 cells. They also inhibit the assembly of purified tubulin *in vitro*, whereas a non-apoptotic PBOX compound (PBOX-21) has no effect on either the cellular microtubule network or on the assembly of purified tubulin. This suggests that the molecular target of the pro-apoptotic PBOX compounds is tubulin. PBOX-6 does not bind to either the vinblastine or the colchicine binding site on tubulin, suggesting that it binds to, an as yet, uncharacterised novel site on tubulin. The ability of PBOX-6 to bind tubulin and cause microtubule depolymerisation, confirms it as a novel candidate for anti-neoplastic therapy.

Molecular Pharmacology Fast Forward. Published on March 29, 2006 as DOI: 10.1124/mol.105.021204
This article has not been copyedited and formatted. The final version may differ from this version.

Microtubules are highly dynamic cytoskeletal fibres that are composed of α/β tubulin and play an important role in many physiological processes, especially in mitosis and cell division. Their importance in mitosis and cell division makes microtubules an important target for anti-cancer therapy (Jordan and Wilson, 2000). The well characterized antimitotic drugs that have proven clinical efficacy, such as the taxanes (paclitaxel, docotaxel) and the *Vinca* alkaloids (vincristine, vinblastine etc.) bind to tubulin. Alternating α and β-tubulin polymerise to microtubules that constitute the mitotic spindles. Microtubule inhibitors disrupt microtubule dynamics of tubulin polymerisation and depolymerisation, which results in the inhibition of chromosome segregation in mitosis and consequently the inhibition of cell division. The three major classes of agents that bind tubulin are the taxanes, which stabilise the microtubules by blocking disassembly, the *Vinca* alkaloids and lastly agents that bind to the colchicine site on tubulin. These latter two classes are microtubule-destabilising agents that act by blocking assembly of tubulin heterodimers.

In the field of antineoplastic chemotherapy, anti-microtubule agents constitute an important class of compounds, with broad activity both in solid tumours and in hematological malignancies. The taxanes are effective in the treatment of refractory ovarian cancer, metastatic breast cancer, non-small cell lung cancer and head and neck and bladder carcinomas (Crown and O'Leary, 2000; Donaldson et al. 1994). The *Vinca* alkaloids have shown clinical benefit in the treatment of leukaemia, Hodgkin's disease, non-Hodgkin's lymphomas, testicular cancer, Kaposi's sarcoma, breast cancer and other malignancies (Jordan and Wilson, 2000). This anti-neoplastic activity is rooted in these compounds' ability to induce mitotic arrest and subsequent apoptotic cell death via the spindle assembly checkpoint. Anti-microtubule agent-induced mitotic arrest is associated with an upregulation and activation of cyclin B_1/CDK1 activity in a variety of cell lines (Donaldson et al. 1994). Studies in both normal and transformed human cells, treated with anti-microtubule agents, have shown that apoptosis can be initiated rapidly and directly from mitotic arrest (Woods et al., 1995; Zhou et al., 2002). In particular, a role for JNK signalling in the apoptotic response of cells to anti-microtubule agents has been suggested. JNK is a member of the mitogen-activated protein kinase family and becomes activated in response to a variety of stressful stimuli including UV-irradiation, growth factor deprivation, heat shock and chemotherapeutic drugs. JNK activity is also increased by anti-microtubule agents in a wide variety of cell types (Lee et al., 1998; Wang et al., 1998; Shtil et al., 1999, Wang et al., 1999), and inhibition of JNK inhibits paclitaxel- (Lee et al., 1998; Wang et al., 1999)), vinblastine- (Brantley-Finley et al., 2003), nocodazole- and colchicine-induced apoptosis (Wang et al., 1998). Because JNK has been implicated primarily in stress responses, JNK activation by anti-microtubule

Molecular Pharmacology Fast Forward. Published on March 29, 2006 as DOI: 10.1124/mol.105.021204
This article has not been copyedited and formatted. The final version may differ from this version.

agents may represent an acute response to microtubule damage. The phosphorylation and thus inactivation of the anti-apoptotic protein Bcl-2 has also been described as an important step from microtubule damage to apoptosis induction (Blagosklonny et al., 1997) and many studies have implicated JNK in the upstream signalling pathway leading to Bcl-2 phosphorylation (Srivastava et al., 1999).

We have previously demonstrated in a series of papers that certain members of a novel series of PBOX compounds potently induce apoptotic cell death in a variety of human chemotherapy resistant cancer cell lines indicating their potential in the treatment of both solid tumours and tumours derived from the haematopoietic system (Zisterer et al., 2000; McGee et al., 2002a; McGee et al., 2002b; McGee et al., 2004). Dissecting the molecular mechanisms underlying PBOX induced apoptosis is fundamental to their development as therapeutic agents in the treatment of cancer. We have shown that activation of JNK is essential during PBOX induced apoptosis (McGee et al., 2002a) and that Bcl-2 phosphorylation is a critical step in the apoptotic pathway induced by a representative PBOX compound, PBOX-6 (McGee et al., 2004). In the present study, we examine the hypothesis that PBOX compounds are microtubule-targeting drugs. We show that PBOX-6 causes an upregulation in CDK1 activity prior to apoptosis. Indirect immunofluorescence analysis demonstrates that pro-apoptotic PBOX compounds cause a depolymerisation of the microtubule network and also inhibit assembly of purified tubulin *in vitro*. This study identifies tubulin as the molecular target of the pro-apoptotic PBOX compounds.

Materials and Methods

Materials. MCF-7 human breast carcinoma breast cells were obtained from ECACC. The pyrrolobenzoxazepines 7-[(dimethylcarbamoyl) oxy]-6-(2-naphthyl)pyrrolo-[2,1-*d*][1,5]benzoxazepine (PBOX-6), 7-[(diethylcarbamoyl)oxy]-6-p-tolylpyrrolo[2,1-*d*][1,5]benzoxazepine (PBOX-21) and pyrrolobenzoxazepine 4-acetoxy-5-(1-(naphthyl)naphtho[2,3-*b*]pyrrolo[2,1-*d*][1,4]oxazepine (PBOX-15) were synthesized as described previously (Campiani et al., 1996) The ApopTag Plus Kit was obtained from Chemicon International Inc. (Temecula, California, USA), the RapiDiff kit was obtained from Diagnostic Developments (Burscough, Lancashire, UK) and the CytoDYNAMIX Screen™3 was obtained from Cytoskeleton Inc. (Denver, Colorado, USA). Colchicine, nocodazole, paclitaxel, vincristine and vinblastine were purchased from Sigma (Poole, Dorset, UK). [^{3}H]Vinblastine was prepared by Amersham Biosciences (Buckinghamshire, UK), and the fluorescein-labelled colchicine was obtained from Cytoskeleton Inc. The PBOX compounds were dissolved in ethanol, whilst the remaining drugs were dissolved in dimethyl

Molecular Pharmacology Fast Forward. Published on March 29, 2006 as DOI: 10.1124/mol.105.021204
This article has not been copyedited and formatted. The final version may differ from this version.

sulfoxide. Control samples were prepared with equivalent volumes of the appropriate solvent. Anti-α-tubulin and FITC-conjugated goat anti-mouse were purchased from Sigma, anti-cyclin A, anti-cyclin B_1 and anti-CDK1 antibodies were obtained from BD Pharmingen (Cowley, Oxford, UK). Anti-JNK antibody was purchased from Santa Cruz (Heidelberg, Germany) and anti-PARP antibody was obtained from Merck Biosciences (Beeston, Nottingham, UK). Histone H1 and GST-c-Jun substrates were purchased from Sigma and Cell Signalling Technology Inc. (Beverly, Massachusetts, USA) respectively. The ECL detection system and [γ^{32}P] ATP were purchased from Amersham Biosciences. Unless stipulated, all other reagents were from Sigma.

Cell Culture. MCF-7 and K-562 cells were grown at 37°C under a humidified atmosphere of 95% O_2 and 5% CO_2. The MCF-7 cells were maintained in MEM whilst the K562 cells were maintained in RPMI 1640 medium. Both media were supplemented with 10% (v/v) FCS, 2mM L-glutamine and 100μg/ml gentamicin (complete medium). The MEM was also supplemented with 1% (v/v) non-essential amino acids.

Flow Cytometric Analysis. Cells were harvested by trypsinisation and following centrifugation were washed with PBS and incubated in ice-cold 70% ethanol in PBS at 4°C. The samples were then centrifuged to remove the ethanol, resuspended in 1ml of staining solution (10μg/ml RNase A, 100μg/ml propidium iodide) and incubated in the dark for 30 min at 37°C. Flow cytometric analysis was performed using a FACSCalibur flow cytometer and CellQuest software (Becton Dickinson).

RapiDiff Staining of Cells. MCF-7 cells were seeded at a density of 1 x 10^5 in a volume of 1ml per well of a 24-well plate. Following treatment with the indicated compounds, a 500μl aliquot of the cells was treated with 1mM EDTA so as to prevent clumping of the cells. The cells were then resuspended thoroughly and cytocentrifuged on to poly-L-lysine coated slides at 700xg for 2 minutes. The slides were stained with the RapiDiff kit (eosin/methylene blue) under conditions described by the manufacturer.

Immunoprecipitation and Kinase Activity Assays. Cells were lysed in IP lysis buffer containing 50mM HEPES, pH 7.5, 150mM NaCl, 1mM EDTA, 2.5mM EGTA, 10% (v/v) glycerol, 0.1% (v/v) Tween 20, 1mM DTT, 1mM NaF, 10mM β-glycerophosphate, and protease inhibitors (10μg/ml leupeptin, 10μg/ml aprotinin, 0.1mM PMSF and 0.1mM sodium orthovanadate). The DTT, NaF, β-glycerophosphate and protease inhibitors were added fresh to the IP buffer. The protein content of the supernatant was determined by Bradford assay. The appropriate antibody (1μg) was added to equal amounts of protein (100-500μg) in each cell lysate sample. The samples were incubated for 3 hours at 4°C. A 50% slurry of

Molecular Pharmacology Fast Forward. Published on March 29, 2006 as DOI: 10.1124/mol.105.021204
This article has not been copyedited and formatted. The final version may differ from this version.

protein A beads in PBS (50μl) was then added to the samples and incubated overnight at 4°C. The samples were then centrifuged for 2 minutes at 500xg and the beads washed. The precipitates were washed 3 times in 1ml of ice-cold IP lysis buffer and then used either for kinase activity assay or resuspended in 20μl of 3X SDS sample buffer and resolved by SDS-PAGE for western blot analysis. For kinase activity assays, following washes with ice-cold IP lysis buffer, the immune-complex beads were washed 3 times with ice-cold kinase buffer which contained the following: 50mM HEPES, pH 7.5, 2.5mM EGTA, 10mM $MgCl_2$, 1mM DTT, 10mM β-glycerophosphate, 1mM NaF and 0.1mM sodium orthovanadate. The kinase reactions were performed by incubating the immunoprecipitates in 30μl of kinase buffer supplemented with 20μM unlabelled adenosine triphosphate (ATP), 2μCi [γ^{32}P] ATP and either 10μg Histone H1 substrate for CDK1 or 1μg of GST-c-Jun substrate for JNK1, and incubating them at 30°C for 30 minutes. The kinase reactions were stopped by resuspending the samples in an aliquot of 3X SDS sample buffer (20μl) and resolved by SDS-PAGE. The gel was dried under a vacuum and exposed to Kodak X-Omat film at -70°C. Phosphorylation was quantitated by densitometric scan analysis using the Scion Image software package of the phosphorylated bands in the autoradiogram (© 2000 Scion Corporation, based on NIH Image for Macintosh).

Western Blot Analysis. Cells were lysed in lysis buffer containing 50mM Tris-HCl, pH 7.5, 250mM NaCl, 5mM EDTA, 0.1% (v/v) Triton, 50mM sodium fluoride, protease inhibitors (1μg/ml aprotinin, 1μg/ml leupeptin, 1μg/ml pepstatin A, 1mM sodium orthovanadate, 100μg/ml PMSF) and 1mM DTT, and the protein concentration of the resultant supernatants were determined by a Bradford assay. For Western blot analysis of PARP, the cells were resuspended in PARP sample buffer (200μl) (62.5mM Tris-HCL pH 6.8, 6M urea, 10% (v/v) glycerol, 2% (w/v) SDS, 0.00125% bromophenol blue and 5% (v/v) β-mercaptoethanol added immediately before use), sonicated for 15 seconds and heated at 65°C for 15 minutes. Equal amounts of lysate was resolved by SDS-PAGE and transferred onto 0.2μm PVDF membrane. The PVDF membrane was blocked in blocking buffer containing 5% (w/v) dry milk in TBST (0.1% (v/v) Tween 20 in TBS) at room temperature for 1-3 hours. Following blocking of the membrane, the immunoblot was incubated in primary antibody overnight at 4°C, and in horseradish peroxidase-labeled secondary antibody for 1 hour at room temperature according to manufacturer's instructions. The immunoblots were analysed using the ECL detection system.

Indirect Immunofluorescence. Cells, seeded upon coverslips were washed gently with 1ml of PBS and fixed in 100% methanol at -20°C for 10 minutes, after which time they were washed three times with PBS.

Molecular Pharmacology Fast Forward. Published on March 29, 2006 as DOI: 10.1124/mol.105.021204
This article has not been copyedited and formatted. The final version may differ from this version.

The cells were then blocked at room temperature for 30 minutes in 5% BSA made up in PBST (0.1% (v/v) Triton in PBS). The cells were incubated for 1 hour at room temperature in primary antibody to α-tubulin, washed 3 times with PBS and then incubated for a further hour at room temperature in FITC-conjugated goat anti-mouse, after which time they were washed a further 3 times with PBS. The cells were then incubated with 0.2μg/ml PI made up in blocking buffer for 2 minutes. To each coverslip, 5μl of a 2μg/ml phenylethylenediamine in a 50:50 solution of PBS and glycerol was applied to the surface of each slide. The slides were then immediately mounted and viewed at a magnification of 1000x with an Nikon microscope and images captured using ImageCapture software.

Tubulin Polymerisation Assay. The assembly of >99% purified bovine tubulin was monitored using the CytoDYNAMIX Screen^{TM}3. Purified bovine brain tubulin was resuspended on ice in ice-cold G-PEM buffer (80mM PIPES pH 6.9, 0.5mM $MgCl_2$, 1mM EGTA, 1mM GTP, 5% (v/v) glycerol) and a 100μl volume (300μg) was pipetted into the designated wells of a half area 96-well plate prewarmed to 37°C. Each compound tested was made up in G-PEM buffer. The assay was conducted at 37°C and tubulin polymerisation was followed turbidimetrically at 340nm in a Spectramax 340PC spectrophotometer (Molecular Devices). The absorbance was measured at 30-second intervals for 1 hour.

Colchicine Tubulin Competition Binding Assay. Each reaction was performed in 0.25mM PIPES buffer at pH 6.9, containing 0.05mM GTP, and 0.25mM $MgCl_2$, containing test compound at the appropriate concentration and >99% purified tubulin stock (1mg/ml). The reaction mixture was mixed gently and incubated at 37°C for 30 minutes, after which time, fluorescent colchicine was added to each reaction giving a final concentration of 0.5μM. This was then incubated for a further 30 minutes at 37°C. Each reaction was then applied to a G25 Sephadex^{TM} chromatography column and the eluate from the columns collected in designated wells of a 96-well plate. When the eluate from the application of the reaction mixture had been collected, 160μl of buffer was applied to the top of the column and the eluate collected in a fresh well. This was continued until 12 wells were filled per reaction. The plate was then read on a Spectramax Gemini XS fluorescence 96-well spectrophotometer (Molecular Devices), at excitation and emission wavelengths of 485nm and 535nm respectively.

Vinblastine Tubulin Competition Binding Assay. The ability of a ligand to bind to the vinblastine-binding site on tubulin was assayed as described for determination of binding to the colchicine-binding site, utilizing a radiolabeled instead of a fluorsecent analogue. The binding of radiolabelled [^{3}H]-vinblastine was used and its presence within the collected fractions measured by liquid scintillation

Molecular Pharmacology Fast Forward. Published on March 29, 2006 as DOI: 10.1124/mol.105.021204
This article has not been copyedited and formatted. The final version may differ from this version.

counting. Each reaction contained a final concentration of 0.5µM [^{3}H]-vinblastine, and >99% purified bovine brain tubulin (1mg/ml). The separation of the bound [^{3}H]-vinblastine from unbound [^{3}H]-vinblastine was achieved using a G50 sephadex^{TM} column.

Results

PBOX-6 Induced Apoptosis is Preceded by an Accumulation of Cells in G2/M. Microtubule-targeting drugs have previously been shown to induce G2/M arrest and apoptosis in many human tumour cells. Fig. II demonstrates that PBOX-6 (Fig. I) induced apoptosis (as measured by the pre-G1 peak in FACS analysis) of human breast MCF-7 and CML K562 cells was preceded by an accumulation of cells in the G2/M phase. Tunel staining and PARP cleavage confirmed that the PBOX-6 induced increase in the pre-G1 peak was due to apoptotic cell death (results not shown). This detailed time course of the changes in distribution of cell cycle phases in response to PBOX-6 treatment also demonstrates that PBOX-6-induced apoptosis was temporally preceded by arrest in the G2/M phase of the cell cycle.

PBOX-6 Induces Morphological Features of Prometaphase Arrest in MCF-7 Cells. Microtubule targeting agents are known to arrest the cell cycle in early mitosis i.e. prometaphase/metaphase. The morphological features of MCF-7 cells were analysed following treatment with PBOX-6 and compared with two representative anti-microtubule agents, paclitaxel and nocodazole as controls (Fig. III). Cells treated with each of the compounds displayed distinct signs of arrest in the prometaphase stage of mitosis as the nuclear membrane has disappeared and the chromatin was condensed. This suggested the PBOX-6 acts as a mitotic inhibitor. Similar results were obtained in K562 cells, indicating that prometaphase arrest induced by PBOX-6 is not restricted to MCF-7 cells (data not shown).

Effect of PBOX-6 on Cyclin B_1 Expression and CDK1 Activity. It was next necessary to determine what effect PBOX-6 treatment had upon CDK1 kinase activity, as it is responsible, through association with its cyclin partner, cyclin B_1, for driving the cell through G2 and mediating both entrance into and exit out of the M phase of the cell cycle. Paclitaxel and nocodazole-induced M-phase arrest is associated with upregulation and activation of cyclin B/CDK1 kinase in a variety of cell lines (King et al., 1994; Wang et al., 1998), thus treatment with these drugs served as a positive control. Treatment with PBOX-6, paclitaxel or nocodazole resulted in a time-dependent increase in CDK1 kinase activity relative to the vehicle control (Fig. IV A, B and C respectively). In order to address the mechanism by which CDK1 activity was being stimulated, the expression levels of both CDK1 and the cyclins known to associate with it, namely cyclin

Molecular Pharmacology Fast Forward. Published on March 29, 2006 as DOI: 10.1124/mol.105.021204
This article has not been copyedited and formatted. The final version may differ from this version.

A and B_1, were determined. There was no alteration in protein expression of either cyclin A or CDK1 prior to or coincident with the increase in CDK1 activity following treatment with any of the compounds (results not shown). Analysis of expression of cyclin B_1 did however reveal a marked increase in cyclin B_1 after treatment with either PBOX-6 (Fig. VA), paclitaxel or nocodazole (Fig. V B), which directly correlated with the increase in CDK1 activity for each of these compounds (see Fig. IV). Immunoprecipitation experiments confirmed that the PBOX-6 induced CDK1 activity was associated with cyclin B_1 (data not shown). Similar results were also obtained in K562 cells, indicating that activation of cyclin B_1/CDK1 kinase caused by PBOX-6 is not restricted to MCF-7 cells (data not shown). Induction of cyclin B_1/CDK1 kinase activity is a hallmark associated with mitotic arrest, confirming the suggestion that PBOX-6 arrests cells in the G2/M phase of the cell cycle.

PBOX-6 Causes a Dose-Dependent Disruption of MCF-7 Cellular Microtubule Network. Anti-microtubule agents are known to target the cellular microtubule network, resulting in aberrant formation of the mitotic spindle, subsequent blockage of the cell cycle in G2/M-phase and apoptotic cell death (Wassmann and Benezra, 2001). Because PBOX-6 markedly blocked the cell cycle in M-phase and induced apoptotic cell death, we tested whether PBOX-6 could directly affect the organization of the microtubule network of cells. MCF-7 cells were treated with either a range of concentrations of PBOX-6 (100nM to 10μM), paclitaxel (1μM), nocodazole (1μM) or with the same volume of vehicle as control. After 16 hours incubation, the microtubule network was visualized by indirect immunofluoresence. The microtubule network in control cells exhibited normal arrangement with microtubules seen to traverse intricately throughout the cell and these cells displayed a normal compact rounded nucleus (Fig. VI A). In contrast, PBOX-6 caused a dose-dependent loss of microtubule network with only a diffuse stain visible throughout the cytoplasm (Fig. VI B-D). These effects are similar to that exerted by nocodazole (Fig. VI E) a known microtubule depolymeriser. Paclitaxel, on the other hand, exerts its effects by stabilising the microtubule network, and resulted in a distinctive rigidity of the microtubules causing them to form microtubule 'bundles' (Fig. VI F).

PBOX-21 (Fig. I) is a non-apoptotic member of the PBOX series of compounds and in fact induces G1 arrest within MCF-7 cells without any associated cytotoxicity (Mulligan et al., 2003). To test the hypothesis that the differential response of the non- and pro-apoptotic subsets of PBOX compounds is based upon their ability to disrupt the microtubule network, the effect of PBOX-21, as well as a second potent pro-apoptotic PBOX compound, PBOX-15 (Fig. I) on the microtubule network of MCF-7 cells was

Molecular Pharmacology Fast Forward. Published on March 29, 2006 as DOI: 10.1124/mol.105.021204
This article has not been copyedited and formatted. The final version may differ from this version.

examined. It was found that, similar to PBOX-6 (10μM), PBOX-15 (1μM) (Fig. VI G) appeared to induce a loss of the microtubule network of the cell. On the other hand, PBOX-21 (25μM) (Fig. VI H), had no effect upon the MCF-7 microtubule network and, as such, PBOX-21 may be considered a negative control. Collectively these results indicated that the microtubule is the intracellular target for pro-apoptotic PBOX compounds such as PBOX-6.

Effect of PBOX-6 on Tubulin Polymerisation *in vitro*. Because PBOX-6 markedly disrupted the cellular microtubule network, we tested whether PBOX-6 could directly affect tubulin, the main component of this network. To test this hypothesis, tubulin polymerisation and depolymerisation *in vitro* were studied at 37°C in a reaction mixture containing purified tubulin and GTP. Results presented in Fig. VII A show that PBOX-6 inhibited the polymerisation of tubulin in a dose-dependent manner, similar to the effect elicited by nocodazole (Fig. VII B). Similar results were obtained with the other representative pro-apoptotic PBOX compound, PBOX-15 (data not shown). Paclitaxel, in agreement with previous reports was shown to promote tubulin polymerisation in a concentration-dependent manner (Fig. VII C). In contrast, PBOX-21 was found to have a negligible effect upon the polymerisation of tubulin *in vitro* relative to the vehicle control (Fig. VII D), in agreement with its lack of effect upon the cellular microtubule network. This again, distinguishes the mechanism of action of the non- and pro-apoptotic subsets of the PBOX compounds, and identifies tubulin as the molecular target of the pro-apoptotic PBOX members.

Lack of Binding of PBOX-6 to the Vinblastine and Colchicine-Binding Sites on Tubulin. As PBOX-6 has been shown to directly bind to and cause depolymerisation of purified tubulin, it was necessary to gain information about the binding site of PBOX-6 on tubulin. To date, only the binding sites of the depolymerisers colchicine (Serrano et al., 1984; Uppuluri et al., 1993; Ravelli et al., 2004) and vinblastine (Rai and Wolff, 1996) on tubulin have been well characterised. Compounds capable of depolymerising tubulin may bind to either of these two sites, or to an as yet uncharacterised novel site on tubulin. Assessment of the binding of PBOX-6 to the colchicine-binding site involved a fluorescence-based assay. Excess unlabelled colchicine (100μM) or nocodazole (10μM), which is known to bind to the colchicine-binding site (Friedman and Platzer, 1978; Uppuluri et al., 1993), displaced the binding of fluorescently labelled colchicine relative to the vehicle control (Fig. VIII A). PBOX-6 at a concentration of 10μM however did not displace the binding of labelled colchicine suggesting that PBOX-6 does not bind to the colchicine-binding site on tubulin.

Molecular Pharmacology Fast Forward. Published on March 29, 2006 as DOI: 10.1124/mol.105.021204
This article has not been copyedited and formatted. The final version may differ from this version.

Next we determined the ability of PBOX-6 to bind to the vinblastine-binding site on tubulin using a [^{3}H]vinblastine displacement assay. As expected, excess unlabelled vinblastine (100μM) and also vincristine (10μM) (which binds to the vinblastine-binding site) were able to displace [^{3}H]vinblastine relative to their vehicle control (0.5% DMSO v/v), causing a reduction in the radioactive signal in the fractions containing tubulin, i.e. fractions 5-9 (Fig. VIII B). In contrast, 10μM PBOX-6 did not cause a reduction of the radioactive signal relative to the PBOX-6 vehicle control in the fractions containing tubulin, suggesting that PBOX-6 does not bind to the vinblastine-binding site. Any residual [^{3}H]vinblastine that did not bind tubulin, or [^{3}H]vinblastine that had been displaced from binding to tubulin by a vinblastine-binding site competitor, was seen to elute between fractions 10 and 30. These combined results from the colchicine and vinblastine displacement assays indicate that PBOX-6 does not bind to the known sites and may have its own novel binding on tubulin.

Discussion

Although a potent member of a novel series of PBOX compounds, PBOX-6, has previously been shown to induce apoptosis in many human tumour cell lines, our knowledge of the mechanism of action by which PBOX-6 induces apoptosis remained incomplete. We have previously shown that activation of JNK is essential during PBOX induced apoptosis (McGee et al., 2002a) and that Bcl-2 phosphorylation is a critical step in the apoptotic pathway induced by a PBOX-6 (McGee et al., 2004), but the molecular target of PBOX-6 remained to be identified. The present study demonstrates that apoptosis induced by PBOX-6 in human MCF-7 and K562 cells, is preceded by a marked G2/M arrest. The cells displayed morphological features that identified a mitotic arrest, specifically in prometaphase. During prometaphase, the DNA chromatin network, which was duplicated in the S period of interphase, begins to twist and fold, eventually forming compacted chromosomes. The nuclear envelope breaks down allowing the nucleoplasmic contents to come into contact with the spindle network, as the cell prepares to align its duplicated chromosomes during metaphase for separation by the mitotic spindle during anaphase (Crespo et al., 2001). The morphological effects elicited by PBOX-6 were similar to that initiated by two microtubule-targeting drugs, paclitaxel and nocodazole, a representative polymeriser and depolymeriser respectively. This is in agreement with previous reports, which show that anti-microtubule agents arrest the cell cycle in prometaphase (Woods et al., 1995; Li and Broome, 1999).

Molecular Pharmacology Fast Forward. Published on March 29, 2006 as DOI: 10.1124/mol.105.021204
This article has not been copyedited and formatted. The final version may differ from this version.

In eukaryotic cells, cell cycle progression is regulated through the activation and inactivation of cyclin-dependent kinases, cyclins, and other regulatory factors. Inappropriate alteration in the expression and/or activation of cyclin-dependent kinases and regulators can lead to blockade of cell cycle progression and induction of apoptosis. It is widely reported that cyclin B_1/CDK1 complexes are involved in the regulation of the G2/M phase and the M-phase transition. Many reports have demonstrated that anti-microtubule drug-induced M-phase arrest, inappropriate accumulation of B type cyclins and activation of CDK1 were associated with the initiation of apoptotic pathways. In the present study, we show that PBOX-6 treatment promoted an increase in cyclin B_1 protein levels and stimulation of CDK1 activity with a pattern similar to that detected for both paclitaxel and nocodazole. As the G2/M arrest profile paralleled the induction of cyclin B_1 expression and CDK1 activity following treatment with PBOX-6, this would suggest that sustained activation of CDK1 kinase activity by this compound is essential for the cessation of the cell cycle at the G2/M phase.

Because PBOX-6 was found to induce many of the hallmarks associated with mitotic arrest in a manner similar to anti-microtubule agents this suggested that PBOX-6 may in fact possess anti-microtubule activity. This hypothesis was tested by assessing the ability of PBOX-6 to interact with the microtubule network of the cell. Indirect immunofluroescence allowed visualization of both the microtubule network and the DNA of the cell. This technique allowed detection of morphological changes in the microtubule network, such as alterations in microtubule organization and arrangement. It also allowed for detection of disruption to the DNA of the cell. It revealed that PBOX-6 possesses anti-microtubule activity, as PBOX-6 treatment disrupted the microtubule network of the cell in a dose-dependent manner. This is in agreement with the dose-dependent induction of mitotic arrest and apoptosis already observed, and suggests that these effects are a direct result of the PBOX-6 mediated abrogation of the microtubule network of the cell. The disruption to the microtubules following treatment with 10μM PBOX-6 was similar to that elicited by the known microtubule depolymeriser, nocodazole. Increasing concentrations of nocodazole and other known tubulin depolymerisers are known to kinetically ‘cap’ the actively growing plus end of microtubules, preventing growth and thus leading ultimately to disassembly of the microtubules (Dumontet and Sikic, 1999). Both PBOX-6 and nocodazole resulted in a dramatic destruction of the microtubule complex network of the cell, relative to the intricate mesh of microtubules witnessed in the vehicle control cells. The effect of PBOX-6 upon the microtubule network was distinct to that elicited by treatment with paclitaxel. Paclitaxel is a known microtubule polymeriser, which with increasing concentration causes an increase in

Molecular Pharmacology Fast Forward. Published on March 29, 2006 as DOI: 10.1124/mol.105.021204
This article has not been copyedited and formatted. The final version may differ from this version.

microtubule mass and a consequential distinctive 'bundling' of the microtubules. It would therefore appear that PBOX-6 targets the microtubule network of the cell, causing its dissolution via microtubule depolymerisation.

In order to address whether the differential response of the non- and pro-apoptotic subsets of PBOX compounds is based upon the ability to distort the microtubule network, the effect upon the microtubule network in MCF-7 cells of PBOX-15, another potent member of the pro-apoptotic subset of PBOX compounds, and PBOX-21, a member of the non-apoptotic PBOX compounds, was assessed. This revealed that PBOX-15 also disrupted the microtubule network of the cell in a manner similar to PBOX-6. In contrast, PBOX-21 had no effect upon the microtubule network of the cell, suggesting that the ability of a PBOX compound to inhibit microtubule polymerisation determines its ability to induce apoptotic cell death.

The disassembly of the microtubule network following treatment with PBOX-6 and PBOX-15 suggested that they act as microtubule depolymerising agents. In order to examine this hypothesis, the effect of PBOX-6 and PBOX-15 upon tubulin assembly in a cell-free system *in vitro* was assessed and compared with the effects of nocodazole and paclitaxel. The effect of PBOX-21 upon the assembly of tubulin *in vitro* was also determined as a negative control. These assays revealed that both PBOX-6 and PBOX-15 inhibits the assembly of tubulin in a dose-dependent manner, confirming them as microtubule depolymerisers. As expected, and in agreement with the literature, nocodazole inhibited tubulin assembly while paclitaxel induced tubulin assembly, both in a dose-dependent fashion. PBOX-21 had a negligible effect upon the assembly of tubulin relative to the vehicle control, once again suggesting that the differential response of members of the anti-proliferative and pro-apoptotic subsets of PBOX compounds is linked to their ability to directly bind to and inhibit the polymerisation of cellular microtubules.

It is notable that both 100nM and 1μM PBOX-6 were capable of inhibiting the assembly of tubulin in the cell-free assay system, whilst these concentrations were found to elicit no effect upon either the microtubule network of the cell or the cell cycle progression. This discrepancy between the concentrations of PBOX-6 that elicit an effect in a cell-free system and cell-based assay is possibly due to compound depletion and/or cell penetration effects. Discrepancies between the concentrations of anti-microtubule agents that elicit effects in cell-based and cell-free systems have been widely reported (Jiang et al., 1998a; Jiang et al., 1998b; Ling et al., 2002).

Although these PBOX compounds are less potent than some anti-microtubule agents such as paclitaxel, which inhibits cancerous cell growth at low nanomolar concentrations (IC_{50} value ~10nM), some of these

Molecular Pharmacology Fast Forward. Published on March 29, 2006 as DOI: 10.1124/mol.105.021204
This article has not been copyedited and formatted. The final version may differ from this version.

novel PBOX compounds, such as PBOX-15, are still effective in the nanomolar range (IC_{50} value ~250nM). PBOX-15 is therefore much more potent than some other anti-microtubule agents such as arsenic trioxide (Ling et al., 2002) and salvinal (Chang et al., 2004) which only elicit effects in the micromolar range (IC50 value ~10 μM for both compounds).

Anti-microtubule compounds can be classified into different categories depending on their binding sites on tubulin. Through the use of techniques such as photoaffinity labelling (Bai et al., 1996a; Bai et al., 1996b; Rai and Wolff, 1996) and protein footprinting experiments (Chaudhuri et al., 2000) as well as the crystal structures identified by Nogales et al. (1998), and more recently by Ravelli et al., (2004) specific binding residues and binding domains upon tubulin have been at least partially characterised for paclitaxel, vinblastine and colchicine. *Vinca* alkaloids, rhizoxin, dolastetins and spongistatin react with the domain for vinblastine. Colchicine, nocodazole, podophyllotoxin and curacin A bind to the colchicine domain (Rai and Wolff, 1996). As these are the only two defined binding sites of tubulin depolymerisers, it was necessary to determine if PBOX-6 mediated its anti-microtubule activity via binding to either of these sites. The results from the competitive binding experiments revealed that PBOX-6 did not inhibit binding of either colchicine or vinblastine to tubulin, indicating that PBOX-6 has its own, novel, binding site upon tubulin. Other anti-microtubule agents such as estramustine (Panda et al., 1997), arsenic trioxide (Ling et al., 2002), naphthopyran (Dell, 1998) and cemadotin (Jordan et al., 1998) have also been shown to bind to as yet uncharacterised novel sites on tubulin.

In conclusion, we have identified tubulin as the molecular target of pro-apoptotic PBOX compounds such as PBOX-6. The clinical efficacy of anti-microtubule agents is well established, although increasing evidence of resistance to these agents has prompted the search for new agents with a similar mechanism. The ability of PBOX-6 both to induce cell death and cell cycle arrest, bind tubulin and cause microtubule depolymerisation identify it as a strong candidate for anti-neoplastic therapy.

Molecular Pharmacology Fast Forward. Published on March 29, 2006 as DOI: 10.1124/mol.105.021204
This article has not been copyedited and formatted. The final version may differ from this version.

References

Bai R, Pei XF, Boye O, Getahun Z, Grover, S, Bekisz J, Nguyen NY, Brossi A and Hamel E (1996a) Identification of cysteine 354 of beta-tubulin as part of the binding site for the A ring of colchicine. *J Biol Chem* **271**:12639-12645

Bai R, Schwartz R E, Kepler J A, Pettit G R and Hamel E (1996b) Characterization of the interaction of cryptophycin 1 with tubulin: binding in the Vinca domain, competitive inhibition of dolastatin 10 binding, and an unusual aggregation reaction *Cancer Res* **56**:4398-4406

Blagosklonny MV, Giannakakou P, el-Deiry WS, Kingston DG, Higgs PI, Neckers L and Fojo T (1997) Raf-1/bcl-2 phosphorylation: a step from microtubule damage to cell death. *Cancer Res* **57**:130-135

Brantley-Finley C, Lyle CS, Du L, Goodwin ME, Hall T, Szwedo D, Kaushal, GP and Chambers TC (2003) The JNK, ERK and p53 pathways play distinct roles in apoptosis mediated by the antitumor agents vinblastine, doxorubicin, and etoposide. *Biochem Pharmacol* **66**:459-469

Campiani G, Nacci V, Fiorini I, De Filippis MP, Garofalo A, Ciani, S M, Greco G, Novellino E, Williams DC, Zisterer, DM, Woods MJ, Mihai C, Manzoni C and Mennini T (1996) Synthesis, biological activity, and SARs of pyrrolobenzoxazepine derivatives, a new class of specific "peripheral-type" benzodiazepine receptor ligands. *J Med Chem* **39**:3435-3450

Chang JY, Chang CY, Kuo CC, Chen LT, Wein YS, and Kuo YH. (2004) Salvinal, a novel microtubule inhibitor isolated from Salvia miltiorrhizae Bunge (Danshen), with antimitotic activity in multidrug-sensitive and -resistant human tumor cells. *Mol Pharmacol* **65**:77-84

Chaudhuri AR, Seetharamalu P, Schwarz PM, Hausheer FH and Luduena RF (2000) The interaction of the B-ring of colchicine with alpha-tubulin: a novel footprinting approach. *J Mol Biol* **303**:679-692

Crespo NC, Ohkanda J, Yen T J, Hamilton AD and Sebti S M (2001) The farnesyltransferase inhibitor, FTI-2153, blocks bipolar spindle formation and chromosome alignment and causes prometaphase accumulation during mitosis of human lung cancer cells. *J Biol Chem* **276**:16161-16167

Crown J and O'Leary M (2000) The taxanes: an update. *Lancet* **355**:1176-1178

Dell CP (1998) Antiproliferative naphthopyrans: biological activity, mechanistic studies and therapeutic potential. *Curr Med Chem* **5**:179-194

Donaldson KL, Goolsby GL, Kiener PA and Wahl AF (1994) Activation of p34cdc2 coincident with taxol-induced apoptosis. *Cell Growth Differ* **5**:1041-1050

Downing KH and Nogales E (1998) New insights into microtubule structure and function from the atomic model of tubulin. *Eur Biophys J* **27**:431-436

Dumontet C and Sikic BI (1999) Mechanisms of action of and resistance to antitubulin agents: microtubule dynamics, drug transport, and cell death. *J Clin Oncol* **17**:1061-1070

Friedman PA and Platzer EG (1978) Interaction of anthelmintic benzimidazoles and benzimidazole derivatives with bovine brain tubulin. *Biochim Biophys Acta* **544**:605-614

Jiang JD, Davis AS, Middleton K, Ling YH, Perez-Soler R, Holland JF and Bekesi JG (1998a) 3-(Iodoacetamido)-benzoylurea: a novel cancericidal tubulin ligand that inhibits microtubule polymerization, phosphorylates bcl-2, and induces apoptosis in tumor cells. *Cancer Res* **58**:5389-5395

Jiang JD, Wang Y, Roboz J, Strauchen J, Holland JF and Bekesi JG (1998b) Inhibition of microtubule assembly in tumor cells by 3-bromoacetylamino benzoylurea, a new cancericidal compound. *Cancer Res* **58**:2126-2133

Jordan MA, Walker D, de Arruda M, Barlozzari T and Panda D (1998) Suppression of microtubule dynamics by binding of cemadotin to tubulin: possible mechanism for its antitumor action. *Biochemistry* **37**:17571-17578

Jordan MA and Wilson L (1998) Cancer microtubules as a target for anticancer drugs. *Nat Rev* 2004:4:253-65

King RW, Jackson PK and Kirschner MW (1994) Mitosis in transition. *Cell* **79**:563-571

Lee LF, Li G, Templeton DJ and Ting JP (1998) Paclitaxel (Taxol)-induced gene expression and cell death are both mediated by the activation of c-Jun NH2-terminal kinase (JNK/SAPK). *J Biol Chem* **273**:28253-28260

Ling YH, Jiang JD, Holland JF and Perez-Soler R (2002) Arsenic trioxide produces polymerization of microtubules and mitotic arrest before apoptosis in human tumor cell lines. *Mol Pharmacol* **62**:529-538

Mc Gee MM, Campiani G, Ramunno A, Nacci V, Lawler M, Williams DC and Zisterer DM (2002a) Activation of the c-Jun N-terminal kinase (JNK) signaling pathway is essential during PBOX-6-induced apoptosis in chronic myelogenous leukemia (CML) cells. *J Biol Chem* **277**:18383-18389

McGee MM, Greene LM, Ledwidge S, Campiani G, Nacci V, Lawler M, Williams DC and Zisterer DM (2004) Selective induction of apoptosis by the pyrrolo-1,5-benzoxazepine 7-[[dimethylcarbamoyl]oxy]-6-(2-naphthyl)pyrrolo-[2,1-d] (1,5)-benzoxazepine (PBOX-6) in Leukemia cells occurs via the c-Jun NH2-terminal kinase-dependent phosphorylation and inactivation of Bcl-2 and Bcl-XL *J Pharmacol Exp Ther* **310**:1084-1095

Mc Gee MM, Hyland E, Campiani G, Ramunn, A, Nacci V and Zisterer DM (2002b). Caspase-3 is not essential for DNA fragmentation in MCF-7 cells during apoptosis induced by the pyrrolo-1,5-benzoxazepine, PBOX-6. *FEBS Lett* **515**:66-70

Mulligan JM, Campiani G, Ramunno A, Nacci V and Zisterer DM (2003) Inhibition of G1 cyclin-dependent kinase activity during growth arrest of human astrocytoma cells by the pyrrolo-1,5-benzoxazepine, PBOX-21. *Biochim Biophys Acta* **1639**:43-52

Nogales E, Wolf SG and Downing KH (1998) Structure of the alpha beta tubulin dimer by electron crystallography. *Nature* **391**:199-203

Panda D, Miller HP, Islam K and Wilson L (1997) Stabilization of microtubule dynamics by estramustine by binding to a novel site in tubulin: a possible mechanistic basis for its antitumor action. *Proc Natl Acad Sci U S A* **94**:10560-10564

Rai SS and Wolff J (1996) Localization of the vinblastine-binding site on beta-tubulin. *J Biol Chem* **271**:14707-14711

Ravelli RBG, Gigant B, Curmi PA, Jourdain I, Lachkar S, Sobel A and Knossow M (2004) Insight into tubulin regulation from a complex with colchicine and a stathmin-like domain. *Nature* **428**:(6979) 198-202

Serrano L, Avila J and Maccioni RB (1984) Limited proteolysis of tubulin and the localization of the binding site for colchicine. *J Biol Chem* **259**:6607-6611

Shtil AA, Mandlekar S, Yu R, Walter R J, Hagen K, Tan TH, Roninson IB and Kong AN (1999) Differential regulation of mitogen-activated protein kinases by microtubule-binding agents in human breast cancer cells. *Oncogene* **18**:377-384

Srivastava RK, Mi QS, Hardwick JM, and Longo DL. (1999) Deletion of the loop region of Bcl-2 completely blocks paclitaxel-induced apoptosis. *Proc Natl Acad Sci U S A* **96**:3775-80.

Uppuluri S, Knipling L, Sackett DL and Wolff J (1993) Localization of the colchicine-binding site of tubulin. *Proc Natl Acad Sci U S A* **90**:11598-11602

Wang TH, Popp DM, Wang HS, Saitoh M, Mural JG, Henley DC, Ichijo H and Wimalasena J (1999) Microtubule dysfunction induced by paclitaxel initiates apoptosis through both c-Jun N-terminal kinase (JNK)-dependent and -independent pathways in ovarian cancer cells. *J Biol Chem* **274**:8208-8216

Wang TH, Wang HS, Ichijo H, Giannakakou P, Foster JS, Fojo T and Wimalasena J (1998) Microtubule-interfering agents activate c-Jun N-terminal kinase/stress-activated protein kinase through both Ras and apoptosis signal-regulating kinase pathways. *J Biol Chem* **273**:4928-4936

Wassmann K and Benezra R (2001) Mitotic checkpoints: from yeast to cancer. *Curr Opin Genet Dev* **11**:83-90

Woods CM, Zhu J, McQueney PA, Bollag D and Lazarides E (1995) Taxol-induced mitotic block triggers rapid onset of a p53-independent apoptotic pathway. *Mol Med* **1**:506-526

Zhou J, Gupta K, Yao J, Ye K, Panda D, Giannakakou P and Joshi HC (2002) Paclitaxel-resistant human ovarian cancer cells undergo c-Jun NH2-terminal kinase-mediated apoptosis in response to noscapine. *J Biol Chem* **277**:39777-39785

Zisterer DM, Campiani G, Nacci V and Williams DC (2000) Pyrrolo-1,5-benzoxazepines induce apoptosis in HL-60, Jurkat, and Hut-78 cells: a new class of apoptotic agents. *J Pharmacol Exp Ther* **293**:48-59

Molecular Pharmacology Fast Forward. Published on March 29, 2006 as DOI: 10.1124/mol.105.021204
This article has not been copyedited and formatted. The final version may differ from this version.

Footnotes

Financial support from Enterprise Ireland and the Higher Education Authority is gratefully acknowledged.

Molecular Pharmacology Fast Forward. Published on March 29, 2006 as DOI: 10.1124/mol.105.021204
This article has not been copyedited and formatted. The final version may differ from this version.

Legends

Fig. I

Structures of pyrrolo-1,5-benzoxazepine (PBOX) compounds

Fig. II

PBOX-6-induced apoptosis is accompanied by G2/M arrest

MCF-7 and K562 cells were treated either with vehicle ((0.5% (v/v) ethanol (Control)) or 10μM PBOX-6 for up to 48 hours. Cells were harvested at the time points indicated as described in the Methods section and the percentage of cells in each phase of the cell cycle, the pre-G1 (A), G1 phase (B), S phase (C) and G2/M phase, were analysed using flow cytometry. The pre-G1 phase represents apoptotic cells. The results represent the mean ± S.E.M of 6 separate experiments.

Fig. III

PBOX-6 treatment induces morphological features of prometaphase arrest in MCF-7 cells

Microscopic analysis of MCF-7 cells was performed following treatment with either vehicle (0.5% (v/v) ethanol (A)), 10μM PBOX-6 (B), 10μM nocodazole (C) or 10μM paclitaxel (D) for 8 hours. Following treatment, cells were centrifuged onto a glass slide and stained using the Rapi Diff kit. The cells were visualised under a light microscope (Nikon) at a magnification of 40X. Scale bar, 10μm. The results shown are representative of 3 separate experiments.

Fig. IV

PBOX-6 induces an upregulation in CDK1 kinase activity in a manner comparable with paclitaxel and nocodazole

Whole cell extracts were prepared from MCF-7 cells following treatment with either 10μM PBOX-6 (A), paclitaxel (B) or nocodazole (C) for the indicated times. Protein (200-500μg) was immunoprecipitated with anti-CDK1 antibody and Protein A beads and then incubated with Histone H1 substrate and γ^{32}P-ATP and resolved by SDS-PAGE. Densitometry was performed on the resultant bands using Scion Image software

Molecular Pharmacology Fast Forward. Published on March 29, 2006 as DOI: 10.1124/mol.105.021204
This article has not been copyedited and formatted. The final version may differ from this version.

with the 0 hours vehicle control set to 100%. The results represent the mean ± S.E.M of 3 separate experiments. Statistical analysis was carried out using Microsoft®Office Excel. * $p<0.05$, ** $p<0.01$ with respect to 0 hours vehicle, Students t-test.

Fig. V

PBOX-6 induces an upregulation in cyclin B_1 expression in a manner comparable with paclitaxel and nocodazole

Whole cell extracts were prepared from MCF-7 cells following treatment with either vehicle (0.5% (v/v) ethanol (1)) or 10μM PBOX-6 (2) for the indicated times. Protein (50μg) was resolved using SDS-PAGE, transferred onto PVDF and probed with anti-cyclin B_1 antibody (A). Results were compared with an immunoblot of samples prepared from MCF-7 cells following treatment with either vehicle (0.5% (v/v) DMSO (1)), paclitaxel (2) or nocodazole (3) for the indicated times (B). The results shown are representative of 4 separate experiments.

Fig. VI

Effect of PBOX-6, PBOX-15, PBOX-21, paclitaxel and nocodazole upon the organisation of MCF-7 cellular microtubule network

MCF-7 cells were treated with either vehicle (0.5% (v/v) ethanol) (A), 100nM, 1μM or 10μM PBOX-6 (B, C and D respectively), 1μM nocodazole (E), 1μM paclitaxel (F), 1μM PBOX-15 (G) or 25μM PBOX-21 (H) for 16 hours. After this time, the medium was carefully removed and the cells fixed in cold methanol. Cells were incubated with monoclonal anti-α-tubulin antibody at room temperature for 1 hour at room temperature, and then incubated with FITC-conjugated anti-mouse secondary antibody for a further hour at room temperature. After washing, the cells were stained briefly with propidium iodide. The organisation of the microtubule network (green) and the cellular DNA (red) was visualised by Nikon PS200 fluorescence microscopy at a magnification of 100X. Scale bar, 10μm. The results shown are representative of 3 separate experiments.

Molecular Pharmacology Fast Forward. Published on March 29, 2006 as DOI: 10.1124/mol.105.021204
This article has not been copyedited and formatted. The final version may differ from this version.

Fig. VII

PBOX-6 causes a dose-dependent depolymerisation of tubulin, whilst PBOX-21 has a negligible effect upon polymerisation status of tubulin

Purified bovine tubulin was incubated at 37°C in the presence of either vehicle (0.5% (v/v) ethanol or DMSO) or the indicated concentrations of PBOX-6 (A), nocodazole (B), paclitaxel (C) or PBOX-21 (D). Tubulin polymerisation was determined by measuring the increase in absorbance over time at 340nm. The results shown are representative of 3 separate experiments.

Fig. VIII

PBOX-6 does not bind to the colchicine or vinblastine-binding site on purified tubulin

Each reaction mixture contained 1mg/ml .99% purified bovine tubulin, 0.25mM PIPES buffer at pH 6.9, containing 0.05mM GTP, and 0.25mM $MgCl_2$, in the presence or absence of either excess unlabelled colchicine (100μM) (A) or vinblastine (B). The colchicine and vinblastine binding assays were performed as described in Materials and Methods. Each reaction mixture contained either 0.5μM FITC-labelled colchicines (A) or 0.5 [^{3}H]vinblastine (B) and was incubated for 30 minutes at 37°C. When evaluating the ability of a test compound to bind to either of these sites, the reaction was performed in the presence or absence of the indicated test compounds (10μM) or the appropriate vehicle control (ethanol for PBOX-6 and DMSO for the other compounds). The data presented is representative of 2 separate experiments.

Molecular Pharmacology Fast Forward. Published on March 29, 2006 as DOI: 10.1124/mol.105.021204
This article has not been copyedited and formatted. The final version may differ from this version.

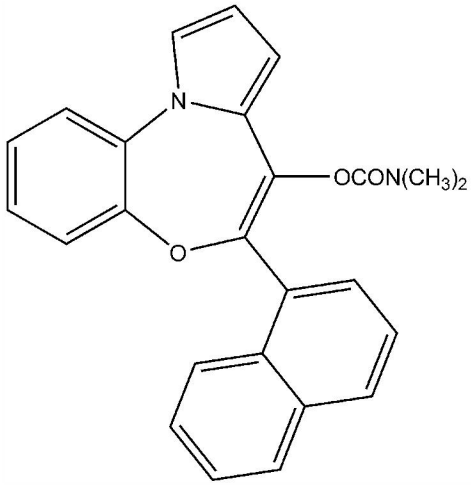

PBOX-6

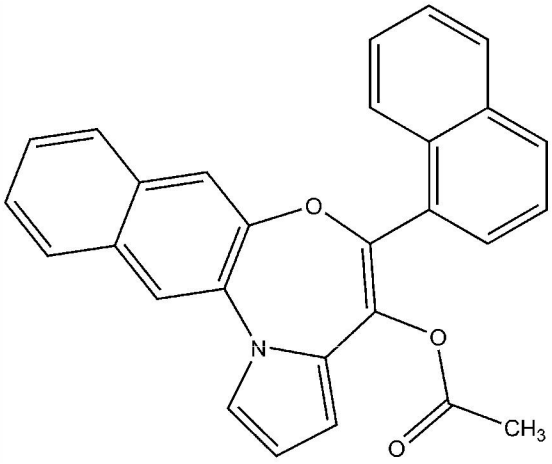

PBOX-15

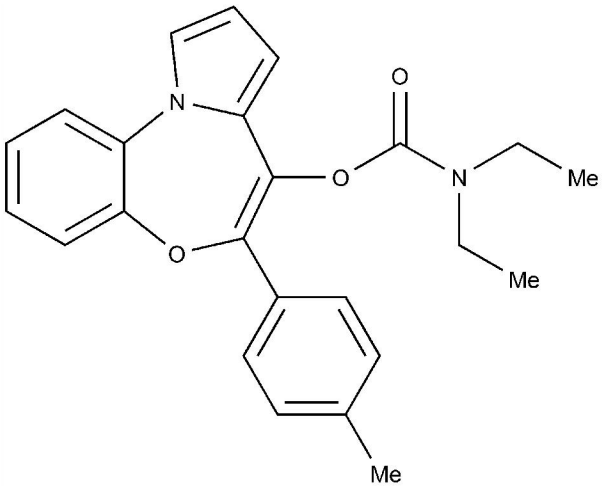

PBOX-21

Figure 1

Molecular Pharmacology Fast Forward. Published on March 29, 2006 as DOI: 10.1124/mol.105.021204
This article has not been copyedited and formatted. The final version may differ from this version.

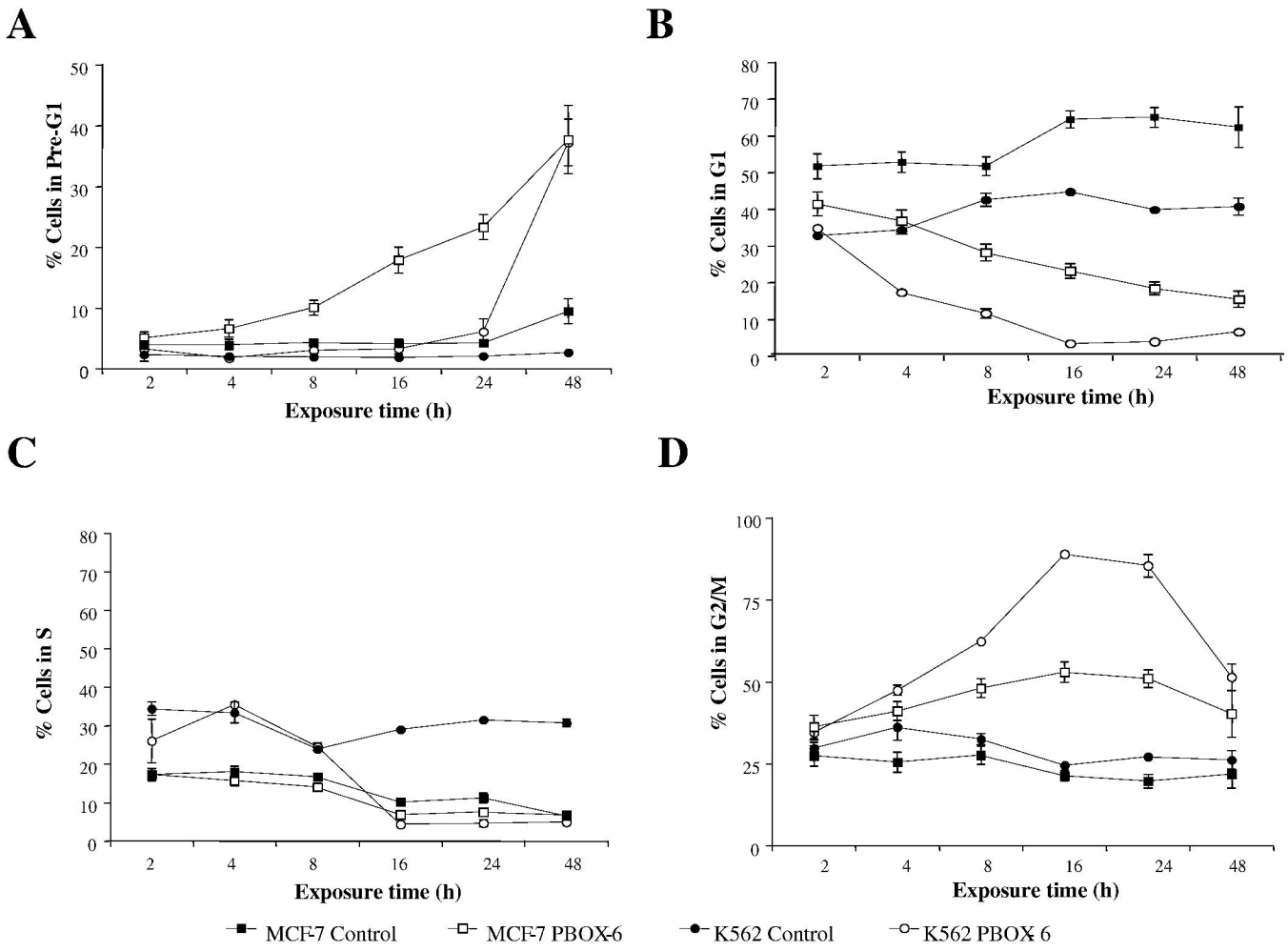

Figure 2

Molecular Pharmacology Fast Forward. Published on March 29, 2006 as DOI: 10.1124/mol.105.021204
This article has not been copyedited and formatted. The final version may differ from this version.

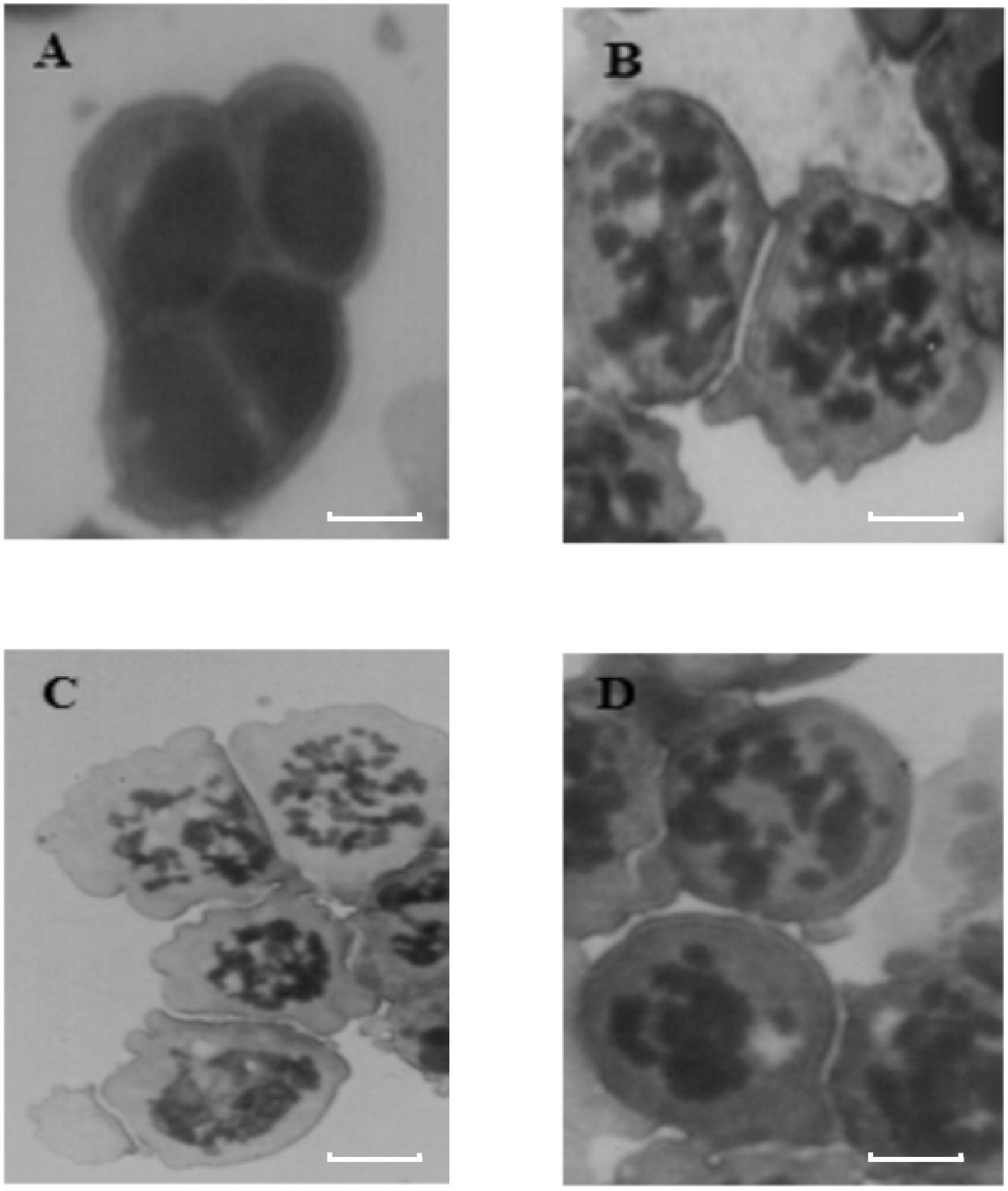

Figure 3

Molecular Pharmacology Fast Forward. Published on March 29, 2006 as DOI: 10.1124/mol.105.021204
This article has not been copyedited and formatted. The final version may differ from this version.

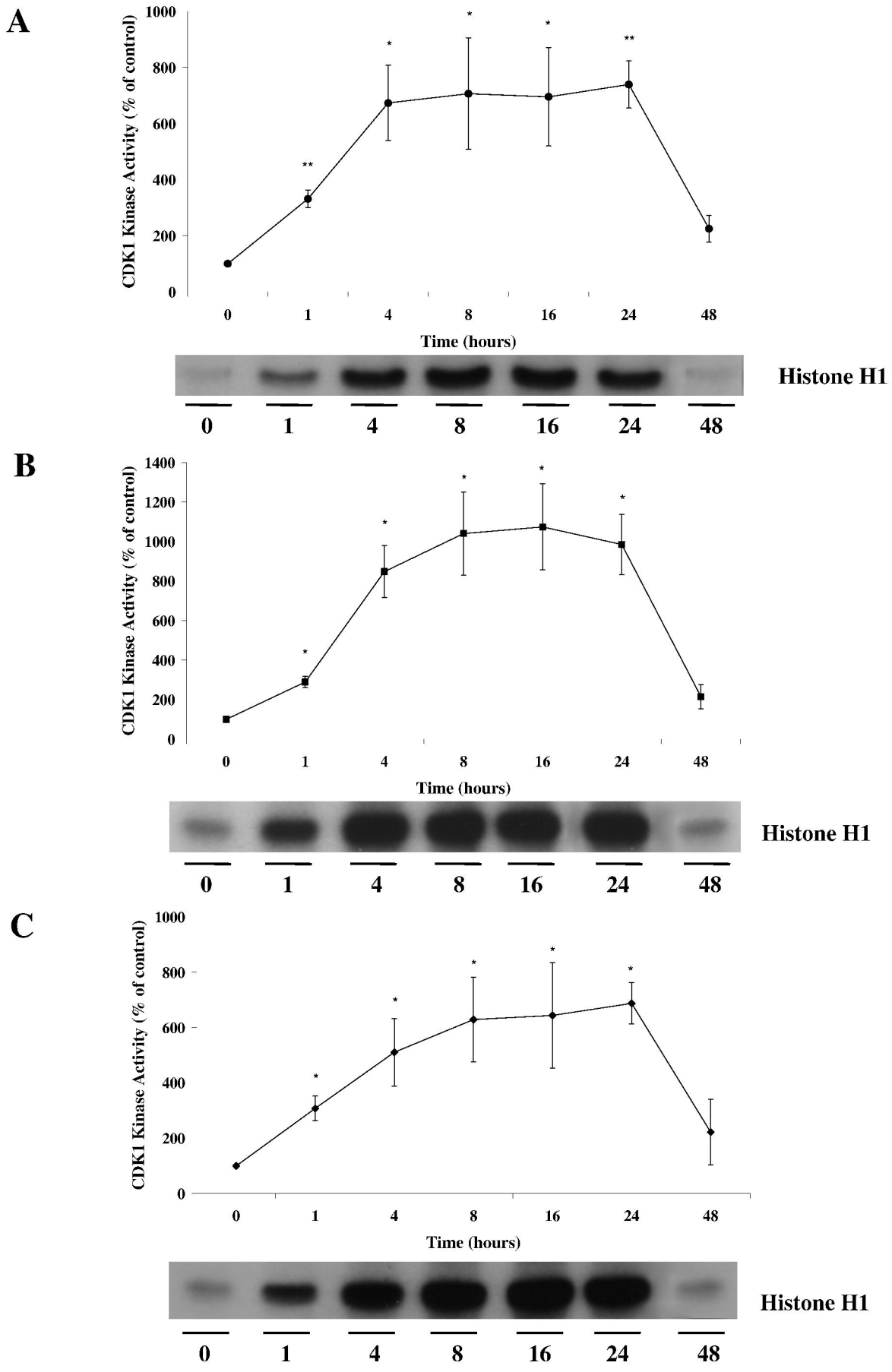

Figure 4

Molecular Pharmacology Fast Forward. Published on March 29, 2006 as DOI: 10.1124/mol.105.021204
This article has not been copyedited and formatted. The final version may differ from this version.

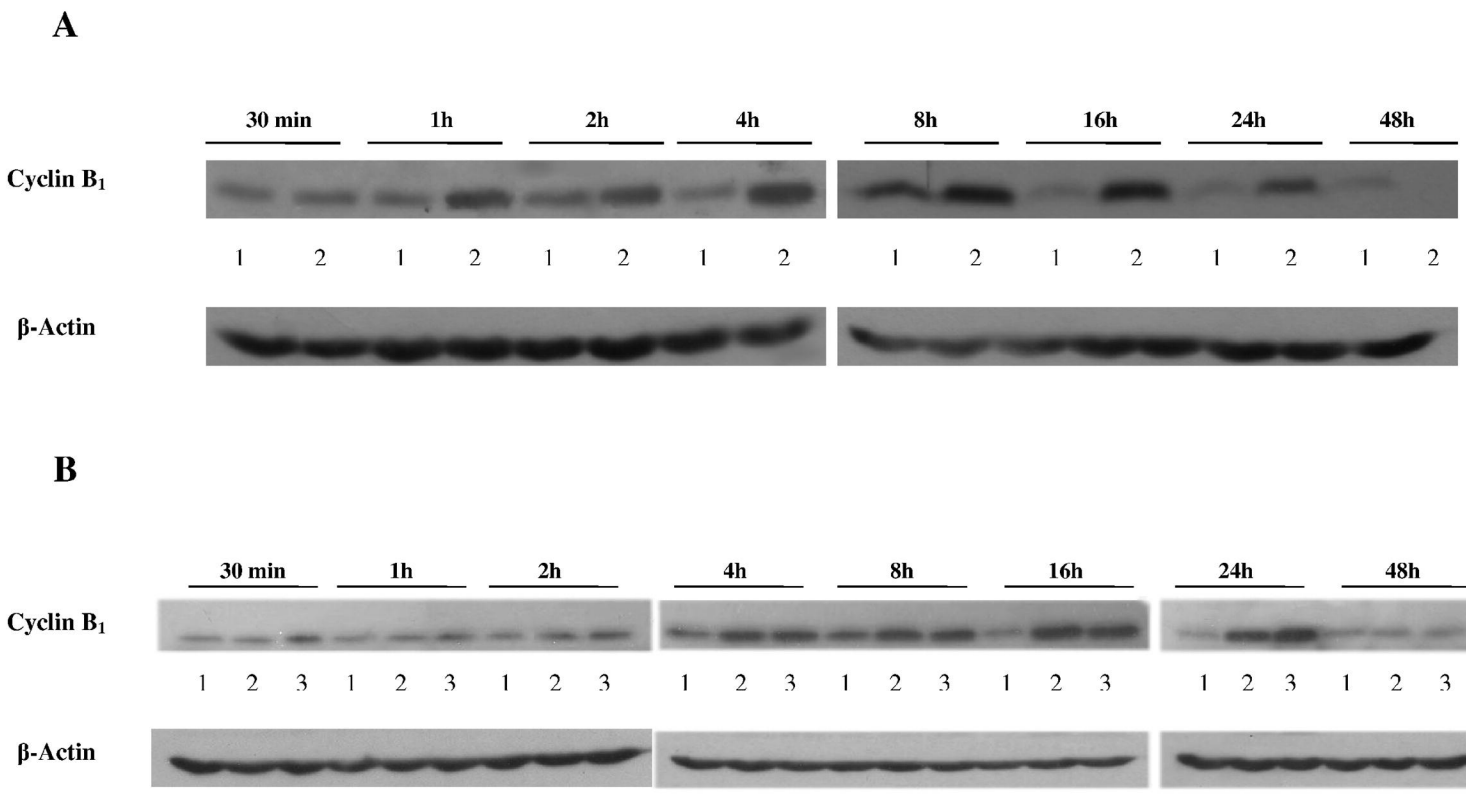

Figure 5

Molecular Pharmacology Fast Forward. Published on March 29, 2006 as DOI: 10.1124/mol.105.021204
This article has not been copyedited and formatted. The final version may differ from this version.

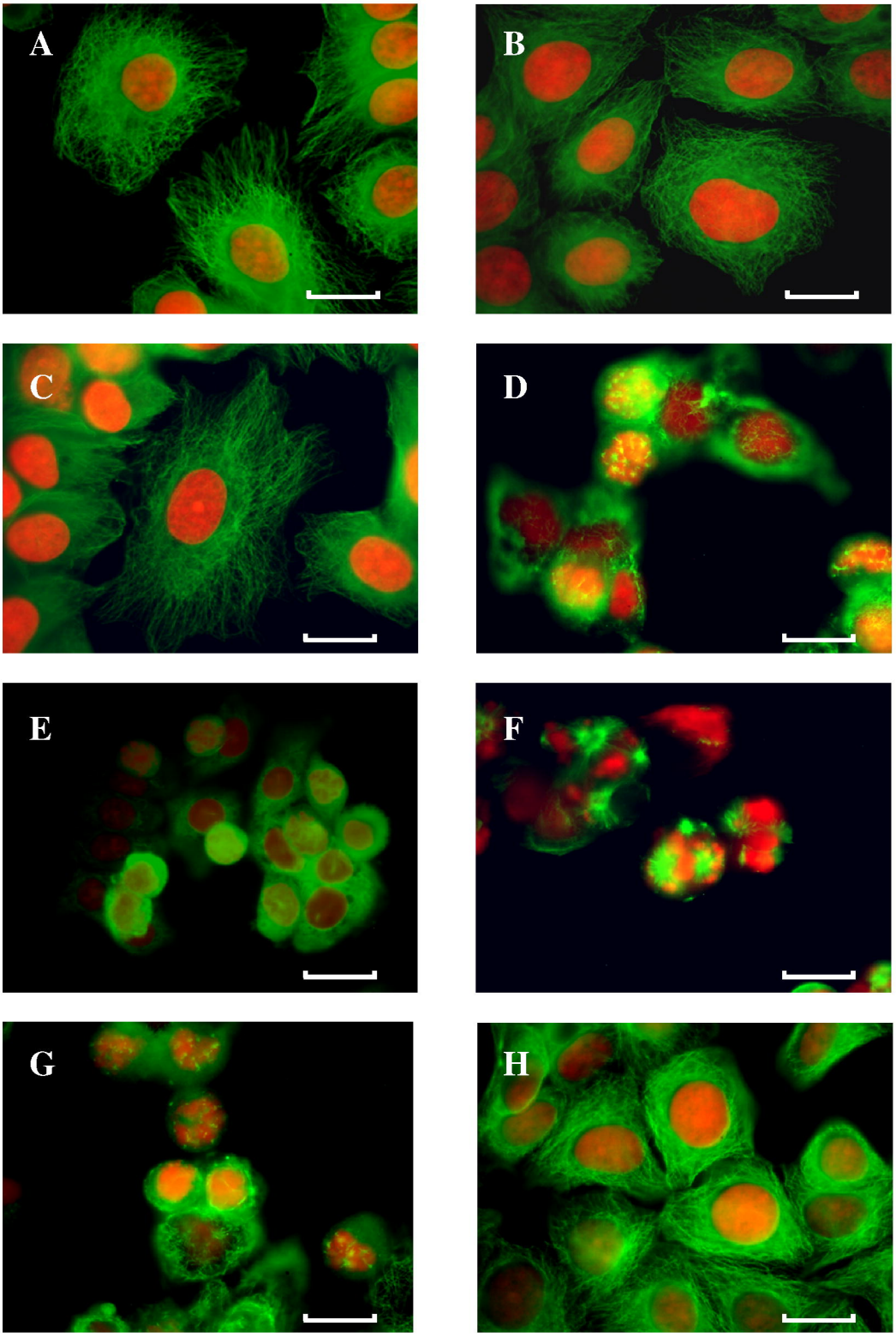

Figure 6

Molecular Pharmacology Fast Forward. Published on March 29, 2006 as DOI: 10.1124/mol.105.021204
This article has not been copyedited and formatted. The final version may differ from this version.

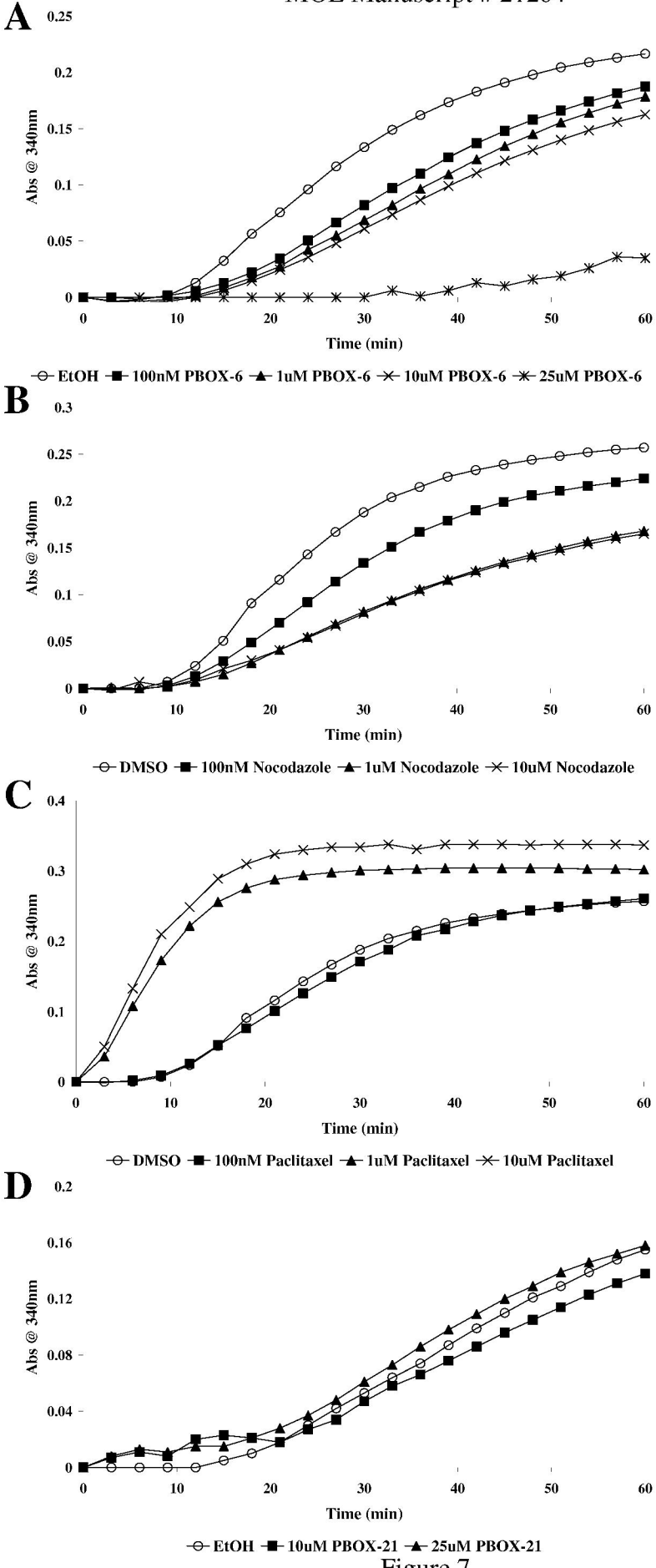

Figure 7

Molecular Pharmacology Fast Forward. Published on March 29, 2006 as DOI: 10.1124/mol.105.021204
This article has not been copyedited and formatted. The final version may differ from this version.

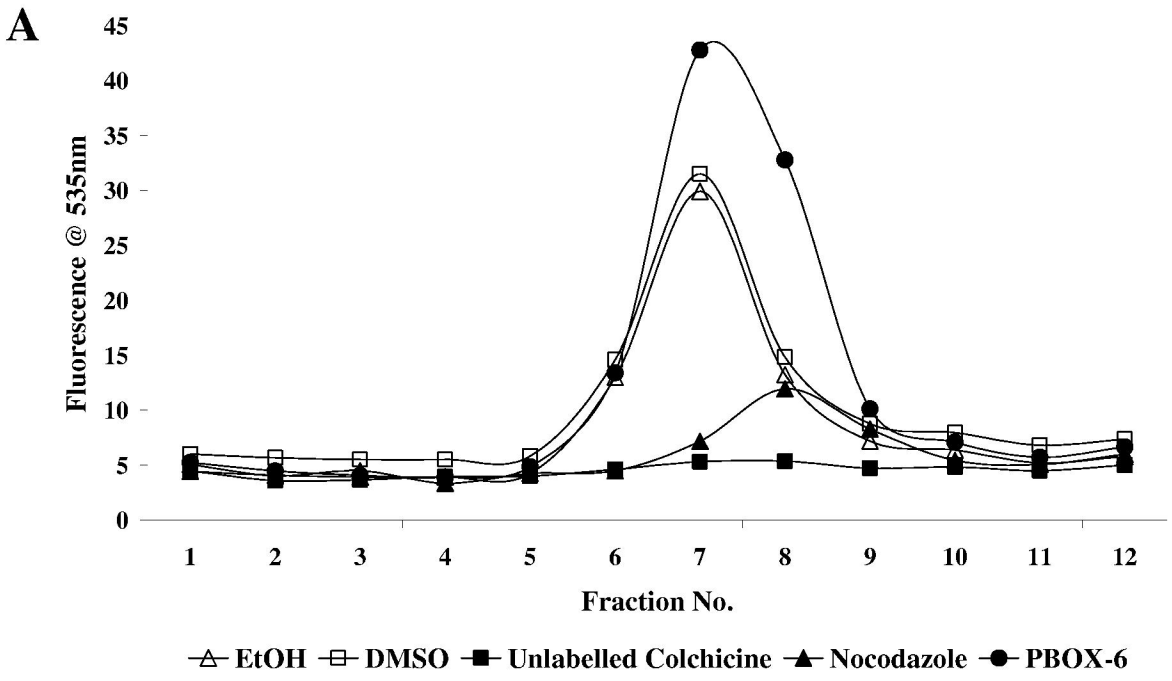

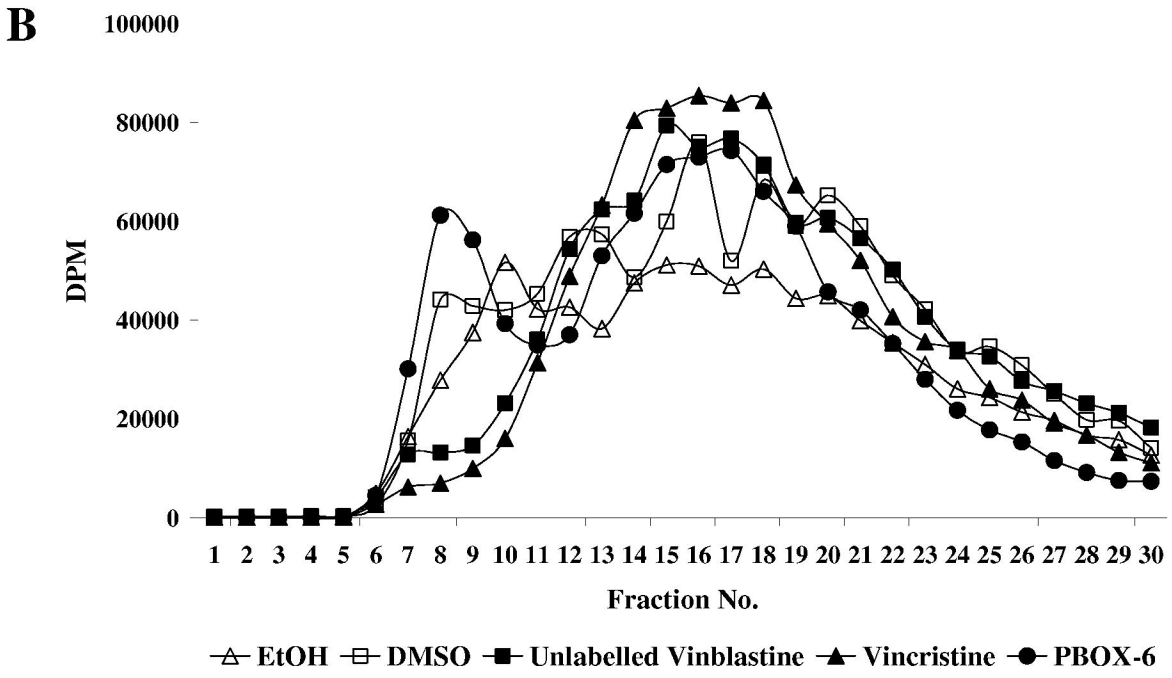

Figure 8